Available online at www.sciencedirect.com
ScienceDirect
Journal of Solid State Chemistry 181 (2008) 263–268
JOURNAL OF SOLID STATE CHEMISTRY
www.elsevier.com/locate/jssc

$La_4(Si_{5.2}Ge_{2.8}O_{18})(TeO_3)_4$ and $La_2(Si_6O_{13})(TeO_3)_2$: Intergrowth of the lanthanum(III) tellurite layer with the XO_4 (X = Si/Ge) tetrahedral layer

Fang Kong[a,b], Hai-Long Jiang[a,b], Jiang-Gao Mao[a,*]

[a]State Key Laboratory of Structural Chemistry, Fujian Institute of Research on the Structure of Matter, Chinese Academy of Sciences, Fuzhou 350002, PR China
[b]The Graduate School of the Chinese Academy of Sciences, Beijing 100039, PR China

Received 15 October 2007; received in revised form 28 November 2007; accepted 29 November 2007
Available online 4 December 2007

Abstract

Two novel lanthanum(III) silicate tellurites, namely, $La_4(Si_{5.2}Ge_{2.8}O_{18})(TeO_3)_4$ and $La_2(Si_6O_{13})(TeO_3)_2$, have been synthesized by the solid state reactions and their structures determined by single crystal X-ray diffraction. The structure of $La_4(Si_{5.2}Ge_{2.8}O_{18})(TeO_3)_4$ features a three-dimensional (3D) network composed of the $[(Ge_{2.82}Si_{5.18})O_{18}]^{4-}$ tetrahedral layers and the $[La_4(TeO_3)_4]^{4+}$ layers that alternate along the b-axis. The germanate–silicate layer consists of corner-sharing XO_4 (X = Si/Ge) tetrahedra, forming four- and six-member rings. The structure of $La_2(Si_6O_{13})(TeO_3)_2$ is a 3D network composed of the $[Si_6O_{13}]^{2-}$ double layers and the $[La_2(TeO_3)_2]^{2+}$ layers that alternate along the a-axis. The $[Si_6O_{13}]^{2-}$ double layer is built by corner-sharing silicate tetrahedra, forming four-, five- and eight-member rings. The TeO_3^{2-} anions in both compounds are only involved in the coordination with La^{3+} ions to form a lanthanum(III) tellurite layer. $La_4(Si_{5.2}Ge_{2.8}O_{18})(TeO_3)_4$ is a wide band-gap semiconductor.

Keywords: Solid state reactions; Crystal structures; Lanthanum(III) tellurite; Layered silicates

1. Introduction

Metal selenites and tellurites can adopt many unusual structures due to the presence of stereochemically active lone pairs that can serve as an invisible structural directing agent [1–4]. The asymmetric coordination geometry adopted by Se(IV) or Te(IV) may also result in noncentrosymmetric (NCS) structures with interesting physical properties, such as nonlinear optical second harmonic generation (SHG), piezoelectricity and ferroelectricity [5–9]. During recent years, metal selenites and tellurites containing additional rigid tetrahedral anionic groups, such as $(PO_4)^{3-}$ and $(BO_4)^{5-}$, have also attracted a lot of research attentions due to their novel open frameworks and interesting physical properties [10–15]. So far, the tetrahedral groups in these compounds are dominated by the phosphates. It is well known that open frameworks of silicates and germanates have found applications in molecular sieves, catalysts, adsorbents, ion-exchangers, etc. [16–19]. We deem that the introduction of the germanate or silicate tetrahedra into the metal tellurite systems may afford new compounds with novel structures and interesting optical properties. So far there are no reports on metal selenites or tellurites containing additional SiO_4 or GeO_4 tetrahedra. Our exploration in the unknown RE–Ge/Si–Te^{IV}–O systems afforded two novel lanthanum(III) tellurites with additional SiO_4 or GeO_4 tetrahedra, namely, $La_4(Si_{5.2}Ge_{2.8}O_{18})(TeO_3)_4$ and $La_2(Si_6O_{13})(TeO_3)_2$. Herein we report their syntheses, crystal structures and characterizations.

2. Experimental section

2.1. Materials and methods

All reagents were obtained from commercial sources and used without further purification. Microprobe elemental analyses on La, Ge, Si and Te elements were performed on a field emission scanning electron microscope (FESEM, JSM6700F) equipped with an energy dispersive X-ray

*Corresponding author at: Fax: +86 591 8371 4946.
E-mail address: mjg@ms.fjirsm.ac.cn (J.-G. Mao).

0022-4596/$ - see front matter © 2007 Elsevier Inc. All rights reserved.
doi:10.1016/j.jssc.2007.11.031

spectroscope (EDS, Oxford INCA). X-ray powder diffraction (XRD) patterns (Cu$K\alpha$) were collected on an XPERT-MPD θ–2θ diffractometer. Thermogravimetric analysis (TGA) was carried out with a NETZSCH STA 449C unit, at a heating rate of 10 °C/min under an air atmosphere. IR spectrum was recorded on a Magna 750 FT-IR spectrometer photometer as a KBr pellet in the range of 4000–400 cm^{-1}. Optical diffuse reflectance spectrum was measured at room temperature with a PE Lambda 900 UV–Visible spectrophotometer. The instrument was equipped with an integrating sphere and controlled by a personal computer. $BaSO_4$ plate was used as a standard (100% reflectance). The absorption spectrum was calculated from reflectance spectrum using the Kubelka–Munk function: $\alpha/S=(1-R)^2/2R$ [20], where α is the absorption coefficient, S is the scattering coefficient which is practically wavelength independent when the particle size is larger than 5 μm, and R is the reflectance.

2.2. Syntheses of $La_4(Si_{5.2}Ge_{2.8}O_{18})(TeO_3)_4$

Colorless plate-shaped single crystals of $La_4(Si_{5.2}Ge_{2.8}O_{18})(TeO_3)_4$ were initially obtained by solid state reaction of La_2O_3 (0.130 g, 0.4 mmol), GeO_2 (0.042 g, 0.4 mmol), TeO_2 (0.156 g, 1.2 mmol) with 0.4 mmol of CsCl as flux in our attempt to synthesize a lanthanum(III) germanate tellurite. The mixture was thoroughly ground and pressed into a pellet, which was then put into an evacuated quartz tube. The quartz tube was heated at 800 °C for 6 days then cooled to 300 °C at 10 °C/h before switching off the furnace. Microprobe elemental analyses on several single crystals indicate the presence of La, Te, Ge and Si elements in a molar ratio of 1.44:1.41:1:1.93. The incorporated Si element was obviously abstracted from the silica tube [21]. These EDS results are in good agreement with those from single crystal X-ray structural analyses (1.42:1.42:1:1.84). Many attempts to prepare a pure lanthanum silicate tellurite have been made but failed, suggesting that the presence of germanium is necessary to stabilize the structure. After proper structural analyses, single phase of $La_4(Si_{5.2}Ge_{2.8}O_{18})(TeO_3)_4$ was prepared by reacting stoichiometric amounts of La_2O_3, GeO_2, SiO_2 and TeO_2 at 960 °C for 6 days.

2.3. Syntheses of $La_2(Si_6O_{13})(TeO_3)_2$

Colorless needle-shaped single crystals of $La_2(Si_6O_{13})(TeO_3)_2$ were initially obtained by solid state reaction of La_2O_3 (0.130 g, 0.4 mmol), SiO_2 (0.096 g, 1.6 mmol) and TeO_2 (0.126 g, 0.8 mmol) at 960 °C for 6 days in our attempts to replace all Ge elements in $La_4(Si_{5.2}Ge_{2.8}O_{18})(TeO_3)_4$ by Si element. A lot of efforts were made to prepare the single-phase product of $La_2(Si_6O_{13})(TeO_3)_2$ by solid state reaction of corresponding stoichiometric mixtures of La_2O_3, SiO_2 and TeO_2 at different temperatures but were unsuccessful. The highest purity of about 90% was obtained by the reaction of a mixture of $La_2O_3/SiO_2/TeO_2$ in a molar ratio of 1:1:6 at 960 °C for 6 days. The major impurity phase is $La_2Te_6O_{15}$ (*Fm3m*) based on XRD powder diffraction study.

2.4. Crystal structure determination for $La_4(Si_{5.2}Ge_{2.8}O_{18})(TeO_3)_4$ and $La_2(Si_6O_{13})(TeO_3)_2$

Data collections for both compounds were performed on a SATURN 70 CCD equipped with Mo$K\alpha$ radiation and graphite monochromator at 293 K. The data sets were corrected for lorentz factor, polarization, air absorption and absorption due to variations in the path length through the detector faceplate. Absorption corrections based on multi-scan technique were also applied [22]. Both structures were solved by the direct methods and refined by full-matrix least-squares fitting on F^2 by SHELX-97 [23]. All atoms were refined anisotropically. Every germanium site in $La_4(Si_{5.2}Ge_{2.8}O_{18})(TeO_3)_4$ was found to be mixed with some silicon contents. The Ge/Si ratios were determined by occupancy factor refinements with equal displacement parameters for each pair of atoms occupying the same site. The refined Si/Ge ratio is in good agreement with that obtained from EDS microprobe element analyses. All three Si sites in $La_2(Si_6O_{13})(TeO_3)_2$ are disordered and each displays two orientations with 50% occupancy each. O(10) is also disordered with 25% occupancy each of the two sites (O(10) and O(10′)). Cell parameters, data collections and refinement parameters are summarized in Table 1. Important bond distances are listed in Table 2.

Table 1
Crystal data and structure refinements for $La_4(Si_{5.2}Ge_{2.8}O_{18})(TeO_3)_4$ and $La_2(Si_6O_{13})(TeO_3)_2$

Formula	$La_4(Si_{5.2}Ge_{2.8}O_{18})(TeO_3)_4$	$La_2(Si_6O_{13})(TeO_3)_2$
Formula weight	1895.58	1005.56
Space group	$P-1$ (No. 2)	$P2_1/c$ (No. 14)
a (Å)	8.150(5)	14.766(9)
b (Å)	12.892(8)	7.318(4)
c (Å)	14.320(8)	8.099(5)
α (deg.)	106.132(9)	90
β (deg.)	90.045(5)	103.05(1)
γ (deg.)	104.270(5)	90
V (Å^3)	1396.8(14)	852.6(9)
Z	2	2
D_{calc} (g cm^3)	4.507	3.917
μ (Mo$K\alpha$) (mm^{-1})	13.391	8.820
Crystal size (mm)	$0.13\times0.10\times0.02$	$0.10\times0.03\times0.02$
F (000)	1677	908
Reflections collected	10,730	6461
Independent reflections	6231 ($R_{int}=0.029$)	1956 ($R_{int}=0.026$)
Observed data [$I>2\sigma(I)$]	3966	1789
Data/restraints/parameters	6227/0/416	1956/0/181
GOF on F^2	0.940	1.080
R_1, wR_2 ($I>2\sigma(I)$)[a]	0.0363, 0.0926	0.0215, 0.0413
R_1, wR_2 (all data)	0.0603, 0.1059	0.0258, 0.0428

[a] $R_1=\sum||F_o|-|F_c||/\sum|F_o|$, $wR_2=\{\sum w[(F_o)^2-(F_c)^2]^2/\sum w[(F_o)^2]^2\}^{1/2}$.

Further details of the crystal structure studies can be obtained from the Fachinformationszentrum Karlsruhe, 76344 Eggenstein-Leopoldshafen, Germany (Fax: +49 7247808666; e-mail: crysdata@fiz-karlsruhe.de), on quoting the depository numbers CSD 417641 and 418559.

Table 2
Selected bond lengths (Å) for $La_4(Si_{5.2}Ge_{2.8}O_{18})(TeO_3)_4$ and $La_2(Si_6O_{13})(TeO_3)_2$

$La_4(Si_{5.2}Ge_{2.8}O_{18})(TeO_3)_4$			
La(1)–O(10)	2.450(6)	La(1)–O(9)#1	2.475(6)
La(1)–O(12)#1	2.529(6)	La(1)–O(17)	2.551(7)
La(1)–O(5)	2.565(6)	La(1)–O(1)#1	2.609(6)
La(1)–O(6)	2.655(6)	La(1)–O(19)#2	2.869(8)
La(1)–O(16)	2.922(8)	La(1)–O(11)#1	2.963(7)
La(2)–O(8)#3	2.438(6)	La(2)–O(19)#4	2.441(7)
La(2)–O(11)#1	2.479(6)	La(2)–O(17)#1	2.537(6)
La(2)–O(6)#5	2.558(6)	La(2)–O(10)	2.576(7)
La(2)–O(6)	2.665(6)	La(2)–O(12)	2.704(6)
La(2)–O(4)#5	3.116(6)	La(3)–O(29)	2.419(6)
La(3)–O(3)#6	2.442(6)	La(3)–O(4)#5	2.489(6)
La(3)–O(28)	2.515(6)	La(3)–O(2)	3.136(7)
La(3)–O(8)#3	2.520(6)	La(3)–O(1)	2.586(6)
La(3)–O(12)	2.627(6)	La(3)–O(7)#3	2.767(6)
La(4)–O(5)#1	2.447(6)	La(4)–O(2)#6	2.489(6)
La(4)–O(3)	2.513(6)	La(4)–O(28)#7	2.545(7)
La(4)–O(7)	2.550(6)	La(4)–O(7)#8	2.601(6)
La(4)–O(1)	2.706(6)	La(4)–O(29)	2.813(7)
La(4)–O(30)	2.925(8)	La(4)–O(9)	3.010(6)
Te(1)–O(2)	1.856(6)	Te(1)–O(3)	1.858(6)
Te(1)–O(1)	1.885(6)	Te(2)–O(4)	1.856(6)
Te(2)–O(5)	1.873(6)	Te(2)–O(6)	1.877(5)
Te(3)–O(8)	1.849(6)	Te(3)–O(9)	1.860(6)
Te(3)–O(7)	1.871(6)	Te(4)–O(10)	1.859(6)
Te(4)–O(11)	1.864(6)	Te(4)–O(12)	1.879(6)
Ge/Si(1)–O(15)	1.632(8)	Ge/Si(1)–O(13)	1.643(7)
Ge/Si(1)–O(21)#9	1.648(7)	Ge/Si(1)–O(14)	1.660(7)
Ge/Si(2)–O(17)	1.619(6)	Ge/Si(2)–O(18)	1.667(6)
Ge/Si(2)–O(15)	1.675(8)	Ge/Si(2)–O(16)	1.688(7)
Ge/Si(3)–O(19)	1.636(7)	Ge/Si(3)–O(14)	1.686(6)
Ge/Si(3)–O(20)	1.699(7)	Ge/Si(3)–O(16)#2	1.704(7)
Ge/Si(4)–O(22)	1.610(7)	Ge/Si(4)–O(21)	1.625(7)
Ge/Si(4)–O(20)	1.625(7)	Ge/Si(4)–O(18)	1.638(6)
Ge/Si(5)–O(24)	1.620(7)	Ge/Si(5)–O(22)	1.633(7)
Ge/Si(5)–O(25)	1.643(8)	Ge/Si(5)–O(23)	1.649(7)
Ge/Si(6)–O(13)#2	1.610(7)	Ge/Si(6)–O(25)	1.627(8)
Ge/Si(6)–O(26)	1.633(6)	Ge/Si(6)–O(27)	1.647(8)
Ge/Si(7)–O(28)	1.612(6)	Ge/Si(7)–O(27)	1.653(7)
Ge/Si(7)–O(24)#10	1.667(7)	Ge/Si(7)–O(30)#3	1.685(7)
Ge/Si(8)–O(29)	1.647(6)	Ge/Si(8)–O(23)	1.687(7)
Ge/Si(8)–O(26)#10	1.698(7)	Ge/Si(8)–O(30)	1.700(7)
$La_2(Si_6O_{13})(TeO_3)_2$			
La(1)–O(1)#1	2.476(3)	La(1)–O(2)#2	2.480(3)
La(1)–O(4)	2.494(3)	La(1)–O(3)#3	2.536(3)
La(1)–O(2)	2.543(3)	La(1)–O(3)#2	2.685(3)
La(1)–O(4)#4	2.700(4)	La(1)–O(3)	2.731(3)
La(1)–O(5)	2.747(6)	La(1)–O(1)#5	3.113(3)
Te(1)–O(1)	1.853(3)	Te(1)–O(2)	1.864(3)
Te(1)–O(3)#2	1.877(3)		
Si(1)–O(6)#6	1.494(4)	Si(1)–O(9)#7	1.572(4)
Si(1)–O(8)#8	1.586(7)	Si(1)–O(11)	1.617(5)
Si(1′)–O(6)#6	1.529(4)	Si(1′)–O(11)	1.556(5)
Si(1′)–O(9)#7	1.590(4)	Si(1′)–O(10′)#9	1.60(1)
Si(1′)–O(10)#9	1.68(1)	Si(2)–O(11)	1.523(5)
Si(2)–O(8)	1.590(7)	Si(2)–O(9)	1.609(4)
Si(2)–O(7)	1.625(4)	Si(2′)–O(11)	1.570(5)
Si(2′)–O(9)	1.571(5)	Si(2′)–O(7)	1.594(4)
Si(2′)–O(10′)	1.63(1)	Si(2′)–O(10)	1.67(1)
Si(3)–O(4)	1.493(4)	Si(3)–O(7)	1.593(4)
Si(3)–O(5)	1.629(6)	Si(3)–O(6)	1.678(4)
Si(3′)–O(4)	1.556(4)	Si(3′)–O(7)	1.598(4)
Si(3′)–O(6)	1.611(4)	Si(3′)–O(5)#5	1.619(6)

Symmetry transformations used to generate equivalent atoms: For $La_4(Si_{5.2}Ge_{2.8}O_{18})(TeO_3)_4$: #1: $-x+1, -y+1, -z+1$; #2: $-x+1, -y, -z+1$; #3: $x+1, y, z$; #4: $x+1, y+1, z$; #5: $-x+2, -y+1, -z+1$; #6: $-x+1, -y+1, -z$; #7: $x-1, y, z$; #8: $-x, -y+1, -z$; #9: $-x, -y, -z+1$; #10: $-x+1, -y, -z$.
For $La_2(Si_6O_{13})(TeO_3)_2$: #1: $-x+1, -y, -z+1$; #2: $-x+1, y+1/2, -z+1/2$; #3: $-x+1, -y, -z$; #4: $x, -y+1/2, z+1/2$; #5: $x, -y+1/2, z-1/2$; #6: $x, y+1, z$; #7: $-x, y+1/2, -z-1/2$; #8: $x, -y+3/2, z+1/2$; #9: $x, -y+3/2, z-1/2$.

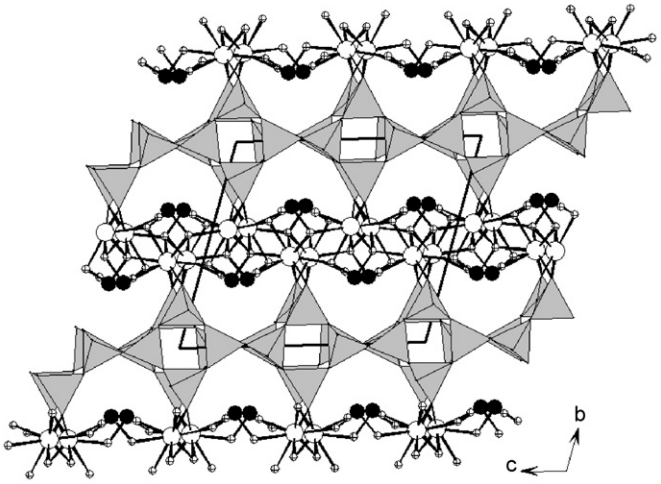

Fig. 1. View of the structure of $La_4(Si_{5.2}Ge_{2.8}O_{18})(TeO_3)_4$ down the *a*-axis. The Si/GeO_4 polyhedra are shaded in light gray. La, Te and O atoms are represented by open, black and crossed circles, respectively.

3. Results and discussion

The structure of $La_4(Si_{5.2}Ge_{2.8}O_{18})(TeO_3)_4$ features a three-dimensional (3D) network built by lanthanide tellurite layers and the silicon/germanium oxide tetrahedral layers (Fig. 1). The asymmetric unit of $La_4(Si_{5.2}Ge_{2.8}O_{18})(TeO_3)_4$ contains four lanthanum(III) cations, eight Si/Ge mixed sites and four tellurite anions. La(1) and La(4) are 10-coordinated by three oxygens from two XO_4 tetrahedra (X = Si, Ge) and seven oxygens from five tellurite groups whereas La(2) and La(3) are surrounded by nine oxygen atoms from two XO_4 tetrahedra (X = Si, Ge) and three monodentate as well as two bidentate tellurite groups. The La–O distances range from 2.420(6) to 3.136(7) Å and the O–La–O bond angles fall in the range of 52.52(16)–164.40(18)°. All tellurium(IV) atoms are ψ-TeO_3 trigonal pyramidal geometry with the pyramidal site occupied by

the lone pair of Te(IV). The Te–O distances fall in the range of 1.850(6)–1.884(6) Å, and O–Te–O bond angles range from 91.1(3)° to 101.8(3)°. These bond distances are comparable to those reported in other lanthanide(III) tellurites [24,25]. Results of bond valence calculations indicate that all tellurium atoms are in +4 oxidation state [26]. The calculated total bond valences are 4.05, 4.10, 4.03 and 4.02 for Te(1), Te(2), Te(3) and Te(4), respectively. The mixed Ge/Si sites are in a slightly distorted tetrahedral geometry with the *X*–O (*X* = Si, Ge) distances of 1.608(7)–1.708(7) Å and O–*X*–O (*X* = Si, Ge) bond angle ranging from 103.5(3)° to 115.2(3)°. These bond distances are comparable to those reported in other lanthanum(III) germanates and silicates [27,28].

The XO_4 (*X* = Si, Ge) tetrahedra are interconnected via corner sharing into a 2D layer parallel to the *ac* plane. Viewing down the *a*-axis, the layer consists of tunnels formed by four-member rings (Fig. 2a). Six-member rings are also found within the 2D layer (Fig. 2b). In the view of topology, $X(1)O_4$, $X(4)O_4$, $X(5)O_4$ and $X(6)O_4$ groups connects with four other XO_4 groups whereas $X(2)O_4$, $X(3)O_4$, $X(7)O_4$ and $X(8)O_4$ groups connects with three other XO_4 groups. Thus, the resultant framework can be described as a (3,4)-connected 2D layer in which the vertex symbols are $6^2.4$ for three-connected XO_4 groups and $6^5.4$ for four-connected XO_4 groups. The $[(Ge_{2.82}Si_{5.18})O_{18}]^{4-}$ layer is related to the $[Si_8O_{18}]^{4-}$ layer in triclinic $K_4(Si_8O_{18})$ [33]. The $[Si_8O_{18}]^{4-}$ layer can also be described as a (3,4)-connected layer with four-, six-, eight-member rings (Fig. 2c). However, these layers are different in that the vertex symbols for three- and four-connected silicate group in the $[Si_8O_{18}]^{4-}$ layer are $4^2.6$ and $4^2.6^4$, respectively. The ratio of 6- to 4-rings in the $[(Ge_{2.82}Si_{5.18})O_{18}]^{4-}$ layer is 4:1 and that in $K_4(Si_8O_{18})$ is 1:2. The $Si_4O_9^{2-}$ anion in hexagonal $K_2Si_4O_9$ and $Ge_4O_9^{2-}$ anions in $BaGe_4O_9$ and $Na_2Ge_4O_9$ feature 3D network structures composed of XO_6 octahedra and XO_4 tetrahedra interconnected by corner- and edge-sharing with the alkaline earth or alkali cations located at the tunnels of the structures [29–32].

The interconnection of the lanthanum(III) ions by the tellurite anions resulted in a lanthanum(III) tellurite layer (Fig. 1). The tellurite anions adopt two types of coordination modes. $Te(1)O_3$ and $Te(2)O_3$ anions each forms a four-member chelating ring with a lanthanum(III) ion and bridges to four other lanthanum(III) ions whereas $Te(3)O_3$ and $Te(4)O_3$ anions each forms two four-member chelating rings with two lanthanum(III) ions and bridges to three other lanthanum(III) ions.

$La_4(Si_{5.2}Ge_{2.8}O_{18})(TeO_3)_4$ can be viewed as formed by the alternately linkage of $[(Ge_{2.82}Si_{5.18})O_{18}]^{4-}$ and $[La_4(TeO_3)_4]^{4+}$ layer via La–O–*X* bridges (*X* = Si, Ge). Semi-circle-shaped channels were formed between the two layers and the lone pairs of Te(IV) are oriented toward the above tunnels (Fig. 1).

The structure of $La_2(Si_6O_{13})(TeO_3)_2$ also features a 3D network also composed of two types of 2D layers, namely lanthanum(III) tellurite layer and the $[Si_6O_{13}]^{2-}$ tetrahedral

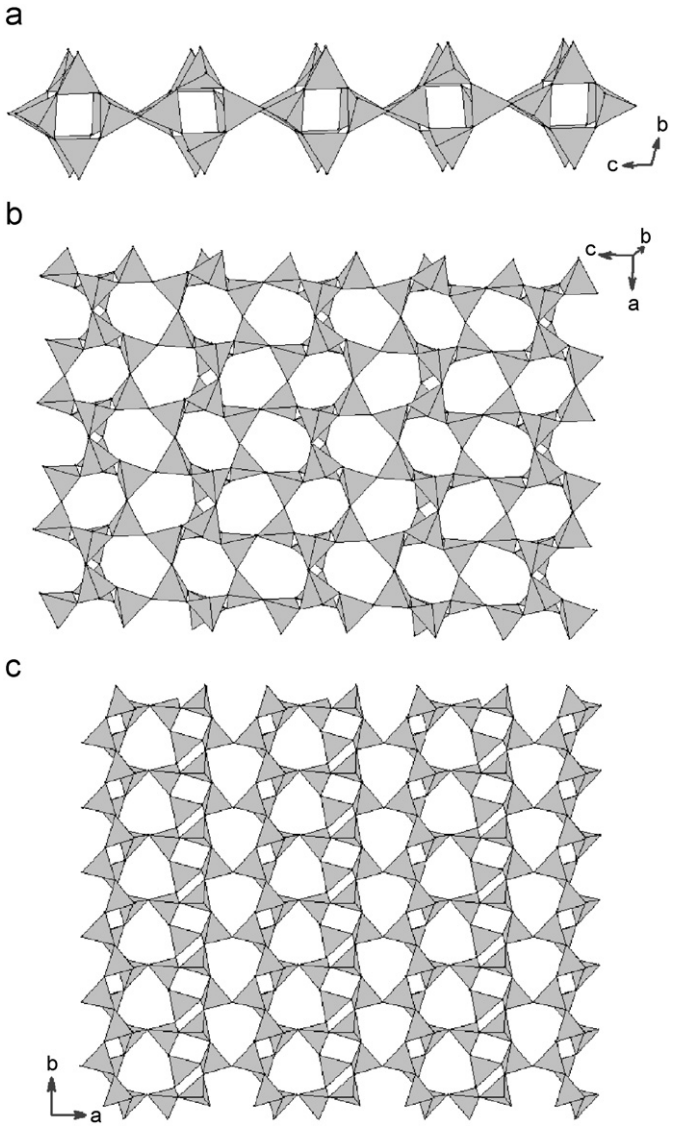

Fig. 2. View of the $[(Ge_{2.82}Si_{5.18})O_{18}]^{4-}$ layer along *a* (a) and *b* (b) axes (*X* = Si, Ge) in $La_4(Si_{5.2}Ge_{2.8}O_{18})(TeO_3)_4$, and view of the $\{Si_8O_{18}\}^{4-}$ layer in $K_4Si_8O_{18}$ along the *c*-axis (c).

double layer (Fig. 3). The asymmetric unit of $La_2(Si_6O_{13})(TeO_3)_2$ contains one unique lanthanum(III) cation, three disordered silicon(IV) and one tellurite anion. The lanthanum(III) ion is 10-coordinated by three oxygen atoms from two silicate groups and seven oxygens from five tellurite anions. The La–O distances range from 2.476(3) to 3.113(3) Å and the O–La–O bond angles fall in the range of 53.85(8)–162.20(9)°. The Te(IV) atom is ψ-TeO_3 trigonal pyramidal geometry with the pyramidal site occupied by the lone pair of Te(IV) as in $La_4(Si_{5.2}Ge_{2.8}O_{18})(TeO_3)_4$. The Te–O distances fall in the range of 1.853(3)–1.877(3) Å, and O–Te–O bond angles range from 92.0(1)° to 100.2(1)°. Results of bond valence calculations indicate that the tellurium atom is in +4 oxidation state. The calculated total bond valence is 4.07 [26]. All three Si(IV) atoms are tetrahedrally coordinated by four oxygen atoms with Si–O distances ranging from 1.493(4) to 1.678(4) Å. These bond

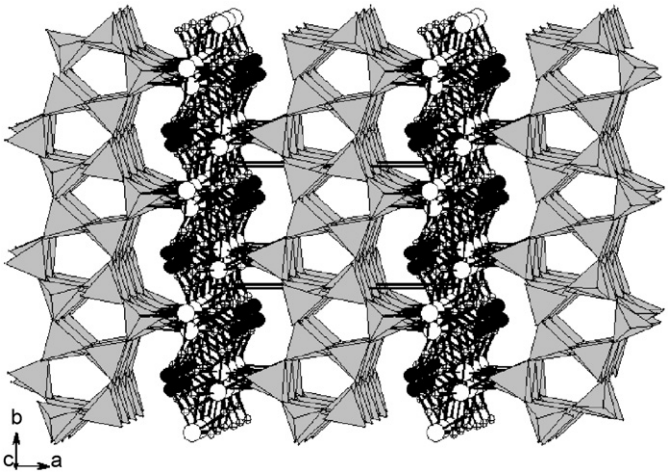

Fig. 3. View of the structure of $La_2(Si_6O_{13})(TeO_3)_2$ down the *c*-axis. SiO_4 polyhedra are shaded in light gray. La, Te and O atoms are represented by open, black and crossed circles, respectively. Only one set of orientations of the distorted silicon atoms were drawn for clarity.

distances are comparable to those in $La_4(Si_{5.2}Ge_{2.8}O_{18})(TeO_3)_4$ and other lanthanum(III) silicates as well as lanthanum(III) tellurites [24,25,38].

The $[Si_6O_{13}]^{2-}$ double layer parallel to the *bc* plane is formed by corner-sharing silicate tetrahedra (Fig. 4). It exhibits 1D channels of five-member rings along the *c* direction (Fig. 5a). In addition, the silicate layer also contains four- and eight-member rings (Fig. 5b). In the view of topology, $Si(3)O_4$ only connects with two other SiO_4 tetrahedra, so they are two-connectors. $Si(1)O_4$ and $Si(2)O_4$ groups are four-connected nodes which can be denoted as $8^3.5^2.4$ mode. To the best of our knowledge, such type of silicate layer has not been reported.

The $[La_2(TeO_3)_2]^{2+}$ layer perpendicular to the *a*-axis is similar to that in $La_4(Si_{5.2}Ge_{2.8}O_{18})(TeO_3)_4$. Unlike that in $La_4(Si_{5.2}Ge_{2.8}O_{18})(TeO_3)_4$, there is only one type of tellurite anion in $La_2(Si_6O_{13})(TeO_3)_2$. The tellurite anion is heptadentate, forming two four-member chelating rings with two lanthanum(III) ions and also bridging with three other lanthanum(III) ions. One oxygen atom is tridentate whereas two other ones are bidentate (Fig. 3).

The above two types of 2D layers are alternatively packed along the *a*-axis and are interconnected via La–O–Si bridges into a 3D network (Fig. 4). Similar to that in $La_4(TeO_3)_4(Ge_{2.815}Si_{5.185}O_{18})$, semi-circle-shaped channels are formed between the two layers and the lone pairs of Te(IV) are oriented toward the above tunnels (Fig. 4).

IR studies indicate that $La_4(Si_{5.2}Ge_{2.8}O_{18})(TeO_3)_4$ is transparent in the range of 4000–1350 cm^{-1}. The absorption bands at 665, 683 and 753 cm^{-1} are characteristic of *v*(Te–O) vibrations, absorption bands at 720, 784, 861 and 1039 cm^{-1} can be assigned to *v*(Si–O) and *v*(Ge–O) vibrations. All of the assignments are consistent with those previously reported [33,34].

$La_4(Si_{5.2}Ge_{2.8}O_{18})(TeO_3)_4$ is thermally stable up to 900 °C (Fig. 5). The weight loss occurred in the range of

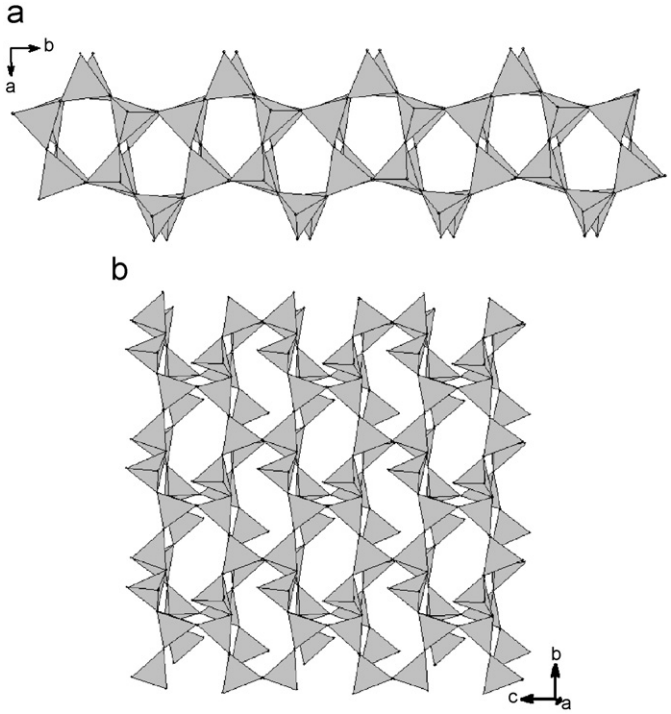

Fig. 4. View of the $[Si_6O_{13}]^{2-}$ double layer in $La_2(Si_6O_{13})(TeO_3)_2$ along *c* (a) and *a* axes (b). The SiO_4 polyhedra are shaded in light gray. Only one set of orientations of the distorted silicon atoms were drawn for clarity.

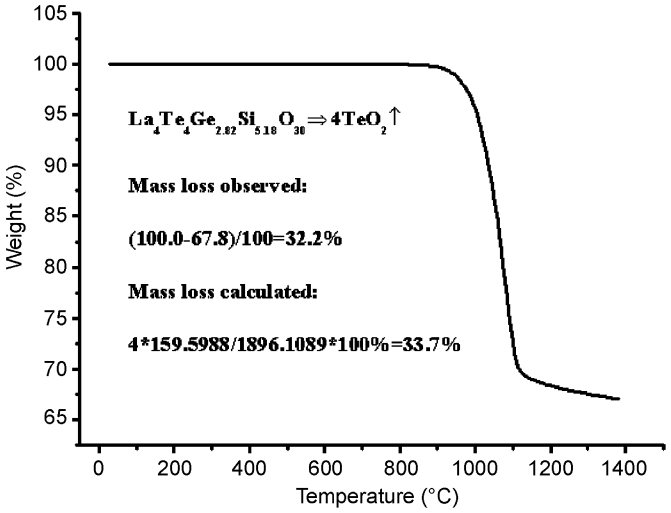

Fig. 5. TGA diagram for $La_4(Si_{5.2}Ge_{2.8}O_{18})(TeO_3)_4$.

900–1100 °C is expected to be due to the release of four TeO_2 molecules per formula unit. The observed weight loss of 32.2% is slightly smaller than the calculated value (33.7%).

Optical diffuse reflectance spectrum of $La_4(Si_{5.2}Ge_{2.8}O_{18})(TeO_3)_4$ reveals an optical band-gap of 4.42 eV (see Supporting materials). Hence, $La_4(Si_{5.2}Ge_{2.8}O_{18})(TeO_3)_4$ is a wide band-gap semiconductor. TGA, IR and optical diffuse reflectance spectrum measurements for $La_2(Si_6O_{13})(TeO_3)_2$ were not performed due to the lack of its pure samples.

Acknowledgments

The authors gratefully acknowledge the financial support from the National Natural Science Foundation of China (Nos. 20731006, 20573113 and 20521101).

Appendix A. Supplementary materials

Supplementary data associated with this article can be found in the online version at doi:10.1016/j.jssc.2007.11.031.

References

[1] M.S. Wickleder, Chem. Rev. 102 (2002) 2011–2087 (and references therein).
[2] M.S. Wickleder, O. Buchner, C. Wickleder, S. el Sheik, G. Brunklaus, H. Eckert, Inorg. Chem. 43 (2004) 5860–5864.
[3] P.-M. Almond, M.-L. McKee, T.-E. Albrecht-Schmitt, Angew. Chem. Int. Ed. 41 (2002) 3426–3429.
[4] M.-S. Wickleder, O. Buchner, C. Wickleder, S. el Sheik, G. Brunklaus, H. Eckert, Inorg. Chem. 43 (2004) 5860–5864.
[5] Y. Porter, K.-M. Ok, N.S.P. Bhuvanesh, P.-S. Halasyamani, Chem. Mater. 13 (2001) 1910–1915.
[6] K.-M. Ok, P.-S. Halasyamani, Chem. Mater. 14 (2002) 2360–2364.
[7] E.-O. Chi, K.-M. Ok, Y. Porter, P.-S. Halasyamani, Chem. Mater. 18 (2006) 2070–2074.
[8] W.T.A. Harrison, L.L. Dussack, A.J. Jacobson, J. Solid State Chem. 125 (1996) 234–242.
[9] V. Balraj, K. Vidyasagar, Inorg. Chem. 38 (1999) 5809–5813.
[10] A. Guesdon, B. Raveau, Chem. Mater. 12 (2000) 2239–2243.
[11] H. Mayer, M. Weil, Z. Anorg. Allg. Chem. 629 (2003) 1068–1072.
[12] K.-M. Ok, J. Orzechowski, P.S. Halasyamani, Inorg. Chem. 43 (2004) 964–968.
[13] F. Kong, S.-P. Huang, Z.-M. Sun, J.-G. Mao, W.-D. Chen, J. Am. Chem. Soc. 128 (2006) 7750–7751.
[14] H. Mayer, Z. Kristallogr. 141 (1975) 354–362.
[15] H. Mayer, G. Pupp, Z. Kristallogr. 145 (1977) 321–333.
[16] D.-W. Breck, Zeolite Molecular Sieves, Wiley, New York, 1974.
[17] E.-M. Flanigen, in Introduction to Zeolite Science and Practice, Elsevier Science, New York, 1991, pp. 13–34.
[18] A. Corma, A. Martinez, Adv. Mater. 7 (1995) 137–144.
[19] N. Dobelin, T. Armbruster, Microporous Mesoporous Mater. 99 (2007) 279–287.
[20] W.M. Wendlandt, H.G. Hecht, Reflectance Spectroscopy, Interscience, New York, 1966.
[21] H.-L. Jiang, J.-G. Mao, Z. Anorg, Allg. Chem. 632 (2006) 2053–2057.
[22] CrystalClear ver. 1.3.5., Rigaku Corp., Woodlands, TX, 1999.
[23] G.M. Sheldrick, SHELXTL, Crystallographic Software Package, SHELXTL, Version 5.1, Bruker-AXS, Madison, WI, 1998.
[24] S.F. Meier, T. Schleid, J. Solid State Chem. 171 (2003) 408–411.
[25] S.F. Meier, T. Schleid, Z. Naturforsch. B 59 (2004) 881–888.
[26] N.E. Brese, M. O'Keeffe, Acta Crystallogr. B 47 (1991) 192–197.
[27] G. Vetter, F. Queyroux, J. Solid State Chem. 73 (1988) 287–297.
[28] S.-M. Wang, S.-J. Hwu, J.A. Paradis, M.-H. Whangbo, J. Am. Chem. Soc. 117 (1995) 5515–5522.
[29] H. Schweinsberg, F. Liebau, Acta Crystallogr. B 30 (1974) 2206–2213.
[30] D.K. Swanson, C.T. Prewitt, Am. Miner. 68 (1983) 581–585.
[31] A. Yu. Shashkov, N.V. Rannev, Yu.N. Venevtsev, Koord. Khim. 10 (1984) 1420–1426.
[32] M.E. Fleet, S. Muthupari, J. Solid State Chem. 140 (1998) 175–181.
[33] Y. Porter, P.S. Halasyamani, Inorg. Chem. 42 (2003) 205–209.
[34] R.A. Nyquist, R.O. Kagel, Infrared Spectra of Inorganic Compounds, Academic Press, New York, London, 1971.